



## Anticancer and antiangiogenic activity of HPMA copolymer-aminohexylgeldanamycin-RGDfK conjugates for prostate cancer therapy

Khaled Greish<sup>a,b,1</sup>, Abhijit Ray<sup>a,b,1</sup>, Hillevi Bauer<sup>a,b</sup>, Nate Larson<sup>a,b</sup>, Alexander Malugin<sup>a,b</sup>, Daniel Pike<sup>a,c</sup>, Mohamed Haider<sup>d</sup>, Hamidreza Ghandehari<sup>a,b,c,\*</sup>

<sup>a</sup> Department of Pharmaceutics and Pharmaceutical Chemistry, University of Utah, Salt Lake City, UT, 84108, USA

<sup>b</sup> Utah Center for Nanomedicine, Nano Institute of Utah, University of Utah, Salt Lake City, UT, 84108, USA

<sup>c</sup> Department of Bioengineering, University of Utah, Salt Lake City, UT, 84108, USA

<sup>d</sup> Department of Pharmaceutics and Industrial Pharmacy, Faculty of Pharmacy, Cairo University, Cairo, Egypt

### ARTICLE INFO

#### Article history:

Received 3 November 2010

Accepted 30 December 2010

Available online 9 January 2011

#### Keywords:

Angiogenesis

Geldanamycin

HPMA copolymer

Prostate cancer

RGDfK

### ABSTRACT

Tumor progression is dependent on neoangiogenesis for blood supply. Neovasculature over-express  $\alpha_v\beta_3$  integrins which recognize the Arg-Gly-Asp (RGD) sequence in the extracellular matrix. *N*-(2-hydroxypropyl)methacrylamide (HPMA) copolymers containing side chains terminated in cyclic RGD analogs such as RGDfK show increased accumulation in prostate tumors. Geldanamycin and their derivatives (e.g., aminohexylgeldanamycin (AH-GDM)) are benzoquinone ansamycins that have both antiangiogenic and antitumor activity. In this work the antiangiogenic and antitumor activities of targetable HPMA copolymer-RGDfK-AH-GDM conjugates were compared with non-targetable systems *in vitro* and *in vivo*. Copolymer-drug conjugates containing RGDfK in the side chains showed superior activity against endothelial and prostate cancer cell lines *in vitro*, as well as higher inhibition of angiogenesis *in vivo*. At equimolar doses of the drug, the RGDfK containing conjugates showed significantly higher antitumor activity in nude mice bearing DU-145 human prostate cancer xenografts. These findings suggest the utility of HPMA copolymer-RGDfK conjugates for targeted delivery of geldanamycin analogs with a dual mode of action.

© 2011 Elsevier B.V. All rights reserved.

### 1. Introduction

Neoangiogenesis is a critical step for tumor growth and development [1]. Newly developed tumor mass usually over-expresses vascular endothelial growth factor (VEGF), which contributes to new blood vessel development. Stable endothelial cells bear vascular endothelial growth factor receptors (VEGFR2), which mediate endothelial cell proliferation and migration in response to elevated levels of VEGF [2–4]. The sprouting endothelial cells further secrete matrix metalloproteinases (MMPs) that digest the surrounding matrix paving the way for the advancing and proliferating endothelial cells. These cells actively extend forward by recognizing specific peptide sequences in basement membrane proteins such as laminin, collagens, and fibronectin [5]. The tripeptide sequence, Arg-Gly-Asp (RGD), has been identified to bind to focal adhesion molecules in endothelial cells such as  $\alpha_v\beta_3$  with high affinity [6]. This binding mediates the attachment of endothelial cells to the basement membrane and signals

intercellular actin fiber rearrangements that lead to endothelial cell migration. Although all endothelial cells use the integrins to anchor to the extraluminal submatrix, the  $\alpha_v\beta_3$  integrin is found on the luminal surface of the endothelial cells primarily during angiogenesis [7]. New vessels provide oxygen and nutrients to the tumor and allow tumor cells to access the circulation, facilitating metastasis.

While tumor cells are largely genotypic and phenotypic heterogeneous, endothelial cells that secure their blood supply are essentially normal with conserved and predictable regulatory mechanisms. Targeting the endothelial cells of neovessels, can cut the life line of tumor tissue, and is an attractive strategy for anticancer treatment. Currently, many angiogenesis inhibitors are being investigated in clinical trials for various cancer treatments [8,9]. Geldanamycin (GDM) is a benzoquinoid ansamycin that binds with high affinity to the chaperone heat-shock protein 90 (HSP90) [10]. HSP 90 is a major regulator of hypoxia-inducible factor (HIF)-1 $\alpha$  [11,12] and vascular endothelial growth factor (VEGF) in the endothelial cells [13], and has nitric oxide mediated proangiogenic effects [14,15]. GDM and their analogs bind to HSP 90, inhibit its ability to fold client proteins into their active conformation and interfere with angiogenesis. In addition, GDM and their analogs interfere with the growth of many tumor tissues including prostate cancer through inactivating essential client protein substrates of HSP 90 [16]. The existence of multiple HSP 90

\* Corresponding author. Department of Pharmaceutics and Pharmaceutical Chemistry, University of Utah, Salt Lake City, UT, 84108, USA. Tel.: +1 801 587 1566; fax: +1 801 585 0575.

E-mail address: [hamid.ghandehari@pharm.utah.edu](mailto:hamid.ghandehari@pharm.utah.edu) (H. Ghandehari).

<sup>1</sup> Both authors contributed equally to this work.

dependent pathways in suppressing both angiogenesis and tumor growth has resulted in a substantial interest in geldanamycin analogs. However clinical development of these drugs has been stalled by poor water solubility and hepatic toxicity. Conjugation of toxic and hydrophobic drugs with macromolecular therapeutics can improve their water solubility and safety [17]. The large size of such systems results in enhanced permeability and retention (EPR) in solid tumors [18]. *N*-(2-hydroxypropyl)methacrylamide (HPMA) copolymers are one example of water-soluble polymeric drug carriers that have been extensively studied for delivery of anticancer and antiangiogenic drugs [19–21]. We have previously demonstrated that attachment of cyclic RGD analogs to HPMA copolymers increases their accumulation in solid tumors of prostate, lung and breast [22], showing their potential for targeted delivery of anticancer drugs and contrast agents. In this work the synthesis, characterization, and antitumor and antiangiogenic activities of HPMA copolymer-RGDfK-AH-GDM conjugates *in vitro* and *in vivo* are reported.

## 2. Materials and methods

### 2.1. Materials

Geldanamycin (NSC 122750) was kindly supplied by the National Cancer Institute Developmental Therapeutics Program (Dr. E. Tabibi). RGDfK (MW 604.5) was obtained from AnaSpec, Inc. (San Jose, CA) at >95% purity and used as supplied. Comonomers of *N*-(2-hydroxypropyl)methacrylamide (HPMA) [23], *N*-methacryloyl glycyglycyl-*p*-nitrophenyl ester (MA-GG-ONp), *N*-methacryloyl-glycyl-phenylalanyl-leucyl-glycine (MA-GFLG-OH) and *N*-methacryloyl-glycylphenylalanyl-leucylglycine-*p*-nitrophenyl ester (MA-GFLG-ONp) were synthesized and characterized according to previously described methods [24,25]. Human Umbilical Vein Endothelial Cells (HUVEC), and prostate cancer cell line DU-145 were obtained from American Type Culture Collection (ATCC, Manassas, VA). DU-145 cells were cultured in RPMI 1640 media (In vitrogen, Carlsbad, CA) supplemented with 4  $\mu$ M-glutamine and 10% (v/v) heat-inactivated fetal bovine serum (FBS). HUVEC cells were cultured in endothelial cell growth media-2 (EGM-2; Lonza, Walkersville, MD). Cell Counting Kit-8 (CCK-8) was used to evaluate cell viability after exposure to different study compounds (Dojindo, Kumamoto, Japan). The basement membrane extract of murine tumor Matrigel (Becton Dickinson Bioscience, San Jose, CA) was used for evaluation of endothelial cell tube formation inhibition. The antiangiogenic effect of the conjugates was quantified *in vivo* using a directed angiogenesis assay kit (Trevigen, Inc., Gaithersburg, MD).

### 2.2. Synthesis and characterization of HPMA copolymer-geldanamycin-peptide conjugates

#### 2.2.1. Synthesis and characterization of drug-containing comonomers

The synthesis of 17-(6-aminohexylamino)-17-demethoxygeldanamycin (AH-GDM), 17-(6-aminohexylamino)-17-demethoxygeldanamycin hydrochloride (AH-GDM.HCl) and *N*-methacryloyl-gly-

cyphenylalanyl-leucylglycyl-17-(6-aminohexylamino)-17-demethoxygeldanamycin (MA-GFLG-AH-GDM) were carried out according to previously described procedures [26]. Resulting products were verified by thin layer chromatography (TLC), mass spectrometry (MS) and nuclear magnetic resonance (NMR) spectroscopy and compared with previously published data [26]. The high resolution mass spectra of comonomer (MA-GFLG-AH-GDM) corresponded to  $C_{57}H_{83}N_8O_{13}$  m/z  $M^{+1}$  (calculated 1087.60796 and found 1087.6089).

#### 2.2.2. Synthesis and characterization of polymeric conjugates

Varying feed comonomer ratios (Table 1) were used for the synthesis of HPMA copolymers via free radical copolymerization in acetone: DMSO [9: 1] using *N*, *N*'-azobisisobutyronitrile (AIBN) as initiator by procedure described previously [27]. Briefly, copolymers P1 (poly(HPMA-co-AH-GDM), the low molecular weight conjugate) and P3 poly(HPMA-co-(MA-GFLG-AH-GDM)-co-(MA-GG-RGDfK)) were synthesized using comonomers of HPMA (0.5 g, 3.477 mmol), MA-GFLG-AH-GDM (0.2588 g, 0.238 mmol), MA-GG-ONp (0.3060 g, 0.952 mmol) and MA-Tyr (0.0237 g, 0.095 mmol) which were dissolved in acetone (5.3 ml) and DMSO (0.6 ml). The ratio of comonomers to initiator to solvent was maintained at 12.5:0.6: 86.9 (w/w/w). The reaction mixture was flushed under nitrogen in a glass ampoule and subsequently sealed. The reaction was carried out in darkness at 50 °C for 24 h. The product was obtained by pouring the reaction mixture into diethyl ether to remove DMSO and assist precipitation of poly(HPMA-co-(MA-GFLG-AH-GDM)-co-(MA-GG-ONp)) (P0). Copolymer P1 conjugate was also prepared as above by the hydrolysis of precursor copolymer P0 to remove the activating group ONp. An aliquot of the polymeric precursor was hydrolyzed using 1.0 N sodium hydroxide (NaOH) to determine the *p*-nitrophenol (ONp) content of released ONp by UV spectrophotometry at 400 nm. HPMA copolymer-AH-GDM-RGDfK conjugate (P3) was synthesized via ONp ester aminolysis of the polymeric precursor (P0). P0 (0.3000 g) was reacted with RGDfK (0.1584 g) in anhydrous DMSO (5 ml) in the presence of pyridine for 24 h followed by the addition of diisopropylethylamine (DIPEA). The reaction mixture was further stirred for 4 h to maximize the attachment of RGDfK. The unreacted ONp was hydrolyzed by slow addition of 0.1 N NaOH (to prevent undesired hydrolysis of drug or targeting moiety) resulting in copolymer P3. Polymer conjugates were dialyzed against distilled water in a regenerated cellulose dialysis membrane of molecular weight cut off (MWCO) 3.5 kDa (Spectrum Laboratories, Inc., Rancho Dominguez, CA) to remove low molecular weight impurities for 72 h.

Samples were further purified by fractionation using size exclusion chromatography (SEC) on a Superose 6 column (10 mm  $\times$  30 cm) (GE Healthcare, Piscataway, NJ) and a Fast Protein Liquid Chromatography (FPLC) system (GE Healthcare) to remove small molecular weight impurities. Peaks that eluted off the column were then monitored via both ultra-violet absorbance (UV), differential refractive index (RI), multi-angle laser-light scattering (MALLS), and quasi-elastic light scattering (QELS) using a DAWN HELEOS II light scattering instrument (Wyatt Technologies, Santa Barbara, CA) with imbedded QELS and an

**Table 1**  
Characteristics of HPMA copolymer conjugates.

Polymer	Feed composition (mol%)				$M_w^a$ (kDa)	Hydrodynamic diameter (nm) <sup>b</sup>	$M_w/M_n^c$	AH-GDM content <sup>d</sup> (wt. %)	Drug per backbone <sup>e</sup>	RGDfK per backbone <sup>f</sup>
	HPMA	MA-GG-ONp	MA-GFLG-AH-GDM	MA-Tyr						
P1	HPMA-GFLG-AH-GDM	73	20	5	22.2	3.2	1.5	19.99	6.88	–
P2	HPMA-GFLG-AH-GDM	93	–	5	38.7	7.3	3.5	26.85	16.11	–
P3	HPMA-GFLG-AH-GDM-RGDfK	73	20	5	18	3.0	1.3	21.80	6.08	8.44
P4	HPMA-RGDfK	78	20	–	20.7	5.0	2.4	–	–	8.57
P5	HPMA	100	–	–	51	8.4	1.13	–	–	–

<sup>a</sup>Estimated by size exclusion chromatography (SEC). <sup>b</sup>Determined by Quasi Elastic Laser Light Scattering. <sup>c</sup>Polydispersity index as a ratio of weight average molecular weight ( $M_w$ ) and number average molecular weight ( $M_n$ ). <sup>d</sup>Drug content as measured by UV spectroscopy. <sup>e</sup>Estimated from molecular weight as calculated by SEC. <sup>f</sup>Determined by amino acid analysis and calculated molecular weight by SEC.

OptiLab rEX differential refractometer (Wyatt Technologies). The Superose 6 column was calibrated with fractions of known molecular weight homopolymers of poly(HPMA). Targeting peptide content of the conjugate was determined by amino acid analysis (University of Utah Core Research Facilities, Salt Lake City, UT). AH-GDM content of the polymeric conjugates was determined by UV spectrophotometry at 340 nm.

The weight average molecular weights of the copolymers ( $M_w$ ) were determined from the simultaneous measurement of the light scattering intensity at 17 angles and of the sample concentration by the refractive index detector. All data was collected and analyzed using Wyatt Technology Corporation Astra 5.3.4.13 light scattering software.

### 2.3. *In vitro* viability assessment

Growth inhibition effect of modified drug (AH-GDM) and the copolymers was evaluated on DU-145 and HUVEC cell lines utilizing CCK-8 assay by pulse chase technique to elucidate the cytotoxic effect of the samples in a time frame equivalent to that of their circulatory half-life as measured previously *in vivo* [28]. 3000 DU-145 or 5000 HUVEC cells per well were seeded in 96-well plates and incubated for 24 h. Cells were then treated with drug and copolymer solutions in complete media for 1.7 h. Subsequently cells were washed twice with buffered phosphate saline and fresh media was added. Following washing of test compounds, cells were further incubated for 72 h. CCK-8 solution was then added at 10  $\mu$ L per well, and the plate was incubated for 1.5 h. Water-soluble tetrazolium salt [2-(2-methoxy-4-nitrophenyl)-3-(4-nitrophenyl)-5-(2,4-disulfophenyl)-2H-tetrazolium, monosodium salt] was reduced by mitochondrial dehydrogenases in active cells resulting in yellow colored water-soluble formazan. The resulting color in active cells was quantified by absorbance at 450 nm using a microplate reader (SPECTRAMax, Molecular Devices). Cell growth inhibition was determined after 72 h incubation and expressed as % cell viability compared to untreated cells. Experiments were conducted in the exponential growth phase.  $IC_{50}$  values were determined by nonlinear regression analysis using GraphPad Prism software.

### 2.4. *In vitro* endothelial tube formation inhibition assay

Growth factor-reduced Matrigel matrix was defrosted over night at 4 °C. 250  $\mu$ L were pipetted in each well of a 24 well plate and four wells were used for each treatment condition. The gel was formed at 37 °C and 5%  $CO_2$  within 30 min. 400  $\mu$ L aliquots of HUVEC cell suspension containing 40,000 cells were then treated with 1.6  $\mu$ M of P1, P3, AH-GDM, or medium (as control). The polymer and cells were both added to the gel, and the plate was further incubated at 37 °C and 5%  $CO_2$  for 24 h. All formed tubes were then counted using 4 $\times$  magnification of inverted microscope attached to Nikon DXM 1200C image capture system, coupled with NJS-Elements F 3.0 image management software (Nikon, Melville, NY). The results are the average of 2 independent experiments.

### 2.5. *In vitro* migration assay

To assess HUVEC migration response to study compounds, the “scratch” wound assay was employed. Cells were seeded into 24-well culture plates previously labeled with traced lines at density of 30,000 cells per well. Once cells were grown to near confluence, the cell monolayer was scratched with a sterile 200  $\mu$ L pipette tip to create a cell-free zone. After wounding, the cells were washed with PBS and cultured in regular growth media supplemented with penicillin/streptomycin (Sigma) with or without 3.2  $\mu$ M of each drug for 24 h. Each treatment was performed in triplicate. At 1 and 24 h after wounding cells were observed under inverted Nikon Diaphot-300 phase-contrast microscope at 100 $\times$  magnification and digitalized

images were captured using Nikon DXM1200C digital camera and ACT-1C 1.01 software (Nikon, Melville, NY). Two images were taken from each well. HUVEC migration was quantified by measuring the area of the cell-free zone with NIH Image J analysis software (v. 1.43). The cell-free area measured at the end of experiment was normalized with the cell-free area measured on images captured 1 h after wounding.

### 2.6. *In vivo* anticancer activity of the conjugates

Six-week-old athymic (*nu/nu*) mice were obtained from Charles River Laboratories (Davis, CA, USA) and used in accordance with the Institutional Animal Care and Use Committee (IACUC) of the University of Utah. Mice were anesthetized using 4% isoflurane mixed with oxygen, and then prostate cancer xenografts were established by subcutaneously injecting  $10 \times 10^6$  DU-145 cells suspended in 200  $\mu$ L of phosphate buffered saline bilaterally on the flank of each mouse.

Tumors were allowed to grow for two weeks to reach average volume of 50 mm<sup>3</sup>, then treatment commenced. Groups of five animals, with a total of ten tumors, were randomly assigned to each study compound. To evaluate the influence of passive targeting on anticancer activity we used three AH-GDM equivalent doses of P1 (Sample with  $M_w$  22.2 kDa, Table 1) and P2 (Sample with  $M_w$  38.7 kDa, Table 1) copolymer conjugates at 10, 20, and 60 mg/kg. Similar doses (10, 20, and 60 mg/kg AH-GDM equivalent) of RGDfK targeted copolymer conjugate (P3, Sample with  $M_w$  18.0 kDa, Table 1) were used to compare active targeting to passive targeting. Unconjugated AH-GDM.HCl was used at a maximum tolerated dose (10 mg/kg) as a positive control, and phosphate buffered saline as a negative control. Animals were weighed and tumor size measured with digital calipers biweekly. The estimated tumor volume ( $V$ ) was calculated using the longitudinal ( $L$ ) and transverse ( $W$ ) cross sections according to the formula:  $V = (L \times W^2)/2$  (expressed in mm<sup>3</sup>). The day of start of the treatments was designated as day 1.

### 2.7. *In vivo* antiangiogenic effect of the conjugates

The antiangiogenic effects of HPMA copolymer-AH-GDM conjugates and appropriate controls were measured using a directed *in vivo* angiogenesis assay kit according to the manufacturer's instructions with modification. Briefly, basement membrane extract with 500 ng/ml VEGF was added in the presence of 7.6  $\mu$ M of copolymer conjugates P1, P2 and P3 and compared with modified drug AH-GDM, and P4 (poly (HPMA-co-(MA-GG-RGDfK))) (Table 1) as control. Study compounds were added in 20  $\mu$ L volume to the angioreactor. The angioreactors were then incubated at 37 °C for 2 h to allow gelation. The angioreactors were subsequently implanted in the dorsal flank of 6- to 7-wk-old female nude mice. After the mice were maintained for 2 weeks, the angioreactors were removed. Basement membrane extract was collected from angioreactors, digested, and centrifuged. The pellets containing the invaded endothelial cells were washed and then labeled with FITC-lectin at 4 °C overnight. After washing, fluorescence was measured in 96-well plates using a SPECTRAMax microplate spectrofluorometer (excitation 485 nm, emission 538 nm; Molecular Devices).

### 2.8. *In vivo* enhancement of tumor permeability in response to the conjugates

DU-145 xenografts were induced in nude mice as described above. When tumor volume reached 50 mm<sup>3</sup>, 10 mg/kg AH-GDM drug equivalent of small, large molecular weight copolymer-drug conjugates (P1 and P2), and targeted small molecular weight copolymer-drug conjugate (P3) were injected via 0.2 ml physiological saline through tail vein *iv* injection. After 18 h, animals were injected with 2 mg Evans Blue Dye (EBD) and 6 h later animals were sacrificed by

CO<sub>2</sub> asphyxiation. Tumors were collected, weighed and incubated with formamide at 37 °C for 72 h to extract EBD from tumor tissues. EBD level per 10 mg tumor weight was quantified as a function of emitted fluorescence at 680 nm (SPECTRAmax, Molecular Devices) when the samples were excited at 620 nm.

### 2.9. Statistical analysis

Differences between means were assessed by student *t* test using Microsoft excel, and GraphPad Prism software. Data was expressed as the mean ± standard error of the mean (SEM). Significant differences were defined as *P* < 0.05, and highly significant *P* < 0.01.

## 3. Results and discussions

### 3.1. Characteristics of HPMA copolymer conjugates

The feed composition and characteristics of HPMA copolymers are summarized in Table 1. AH-GDM containing copolymers, i.e., P1 poly(HPMA-co-(MA-GFLG-AH-GDM)-co-(MA-GG-OH)), (low molecular weight), P2 poly(HPMA-co-(MA-GFLG-AH-GDM)-co-(MA-GG-OH)), (high molecular weight) and P3 poly(HPMA-co-MA-GFLG-AH-GDM)-co-(MA-GG-RGDfK), used a lysosomally degradable tetra peptide linker glycylphenylalanylleucylglycine to conjugate the drug with the polymer backbone while the targeting peptide RGDfK was conjugated with the non degradable dipeptide glycylglycine. The absence of MA-GG-ONp during the synthesis of one of the non-targeted copolymers resulted in the formation of the high molecular weight polymer as ONp acts as a free radical quenching agent. The molecular weights were estimated by SEC. The SEC estimation was by calibrating the Superose 6 column using HPMA homopolymers of molecular weights 17 kDa, 27 kDa, 51 kDa, 95 kDa, 132 kDa, 200 kDa, and 300 kDa. The estimated weight average molecular weight of P1, P2 and P3 was 22.2 kDa, 18.05 kDa and 38.7 kDa with a poly dispersity index of 1.37, 1.91 and 1.30 respectively. Light scattering data also indicated the formation of small mass fraction (<2%) of macromolecules which had molecular weights in excess of 10<sup>6</sup> Da. The hydrodynamic diameter as estimated by QELS for the three copolymers was 3.2 nm, 7.2 nm and 3.0 nm for P1, P2 and P3 copolymers respectively. It is important to note that QELS uses the Stokes–Einstein equation to calculate the hydrodynamic volume for a perfect sphere and thus slightly overestimates the hydrodynamic volume for the linear polymer. The AH-GDM drug contents of 19.99, 26.85 and 21.8 (%wt/wt) respectively were measured spectrophotometrically. Following attachment of RGDfK peptide to the polymeric precursor, P3 and P4 copolymers had an RGDfK peptide content of 0.469 mmol/g and 0.414 mmol/g respectively (Fig. 1).

### 3.2. In vitro growth inhibition assay

In this study DU-145 cells were exposed to polymer-drug conjugates for a time period that corresponds to plasma half life of the copolymers in an attempt to mimic the actual exposure time *in vivo*. At the end of incubation period cells were washed with phosphate buffered saline and incubation continued in fresh medium without drugs. HUVEC cells were treated similarly however none of the study compounds were able to exert growth inhibition at the highest concentration used under study conditions (data not shown). As shown in Fig. 2, the RGDfK targeted copolymer P3 showed the highest cytotoxicity compared to both the modified drug (AH-GDM) and untargeted P1 constructs after the brief period of 1.7 h exposure. The P3 showed 1.4 fold higher activity compared to the free AH-GDM after the short 1.7 h exposure time, possibly due to the recognition of the RGD moiety of the construct by  $\alpha_v\beta_3$  integrins that are frequently expressed on DU-145 cell surface [29]. Thus after rapid washing of various drug conjugates the targeted construct is expected to remain

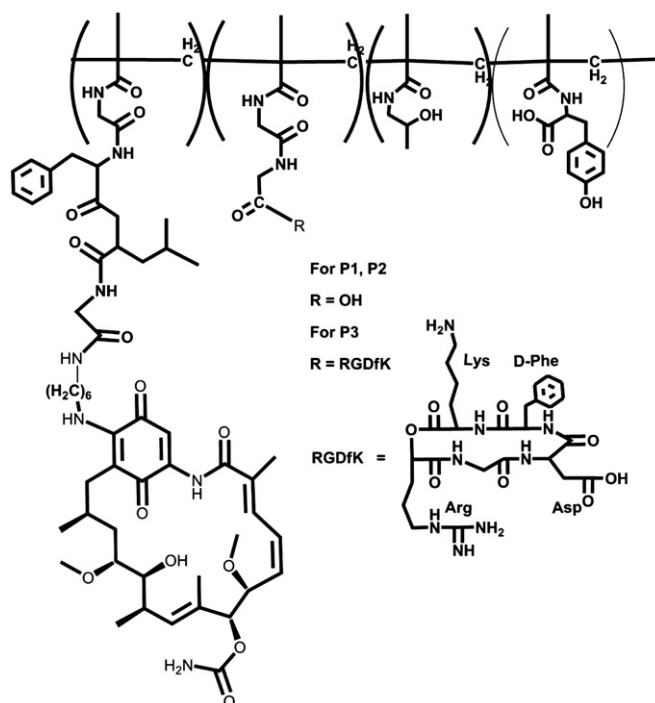


Fig. 1. Structure of HPMA copolymer-AH-GDM-RGDfK conjugates. Copolymers contained the monocyclized RGDfK targeting moiety to target the  $\alpha_v\beta_3$  integrin with aminohexyl geldanamycin in the side chains.

attached to the cell surface while free, and untargeted drugs would be removed. Similar to the washing step *in vitro*, *in vivo* the rapid renal clearance of unconjugated drug would minimize the exposure time of prostate cancer cells to AH-GDM, with clear advantage of the constructs with RGDfK in the side chains.

### 3.3. In vitro endothelial cell tube formation assay

HUVECs have the capacity to form new blood vessels under appropriate conditions, namely the presence of a basement membrane matrix in which specific moieties such as RGD are recognized and function as anchoring points for cell migration and shape

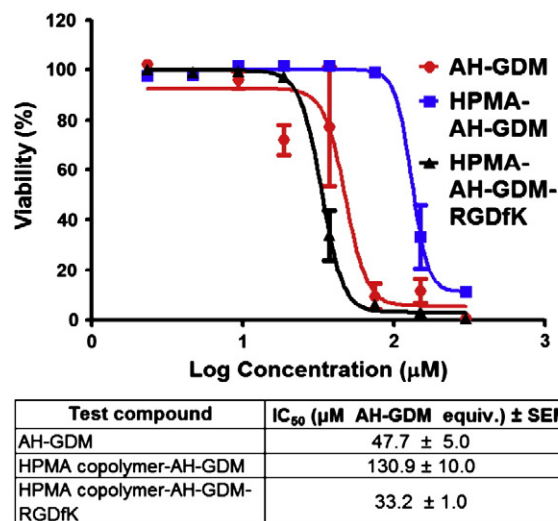
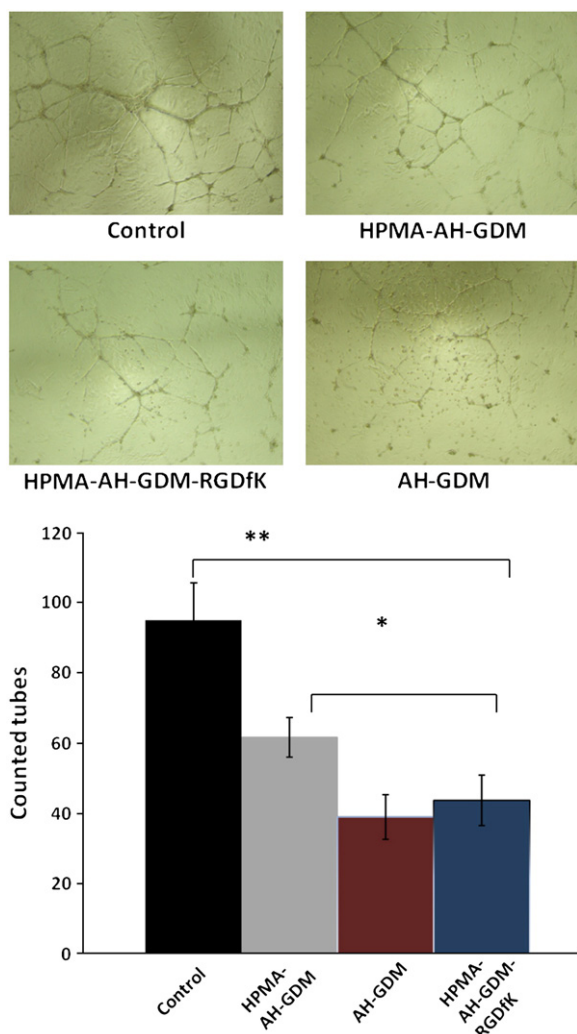


Fig. 2. *In vitro* pulse chase growth inhibition of RGDfK targeted HPMA copolymer-AH-GDM compared to free and untargeted polymer constructs after short exposure to the drugs. Targeted construct shows the highest growth inhibition activity 2–8 fold higher than untargeted polymer-drug conjugate. For sample characteristics see Table 1.

metamorphosis [30]. Angiogenic stimuli (VEGF and FGF) are essential for endothelial cell proliferation and the specific make up of new vessels by endothelial cells. In this study we used Matrigel which is basement membrane extract of murine tumor supplemented with essential endothelial cell growth factors to challenge tube formation in the presence of different AH-GDM polymeric conjugates. As shown in Fig. 3, when HUVEC cells were exposed to 1.6  $\mu\text{M}$  AH-GDM drug equivalence (3% of AH-GDM  $\text{IC}_{50}$ ), the RGDfK targeted conjugate P3 showed a significantly more potent inhibition of tube formation compared to non-targeted polymer-drug conjugates for the same dose. Even though the dose selected for this assay was far from that can cause cell death, functional impairment in the ability of endothelial cells to migrate, differentiate and proliferate as collectively measured by the number of tubes formed were clearly accentuated by the addition of RGDfK moiety. This accentuated impairment can be explained either due to a higher degree of AH-GDM internalization resulting from facilitated receptor mediated endocytosis, or due to the effect of the RGDfK moiety on endothelial cell response to VEGF through limiting VEGFR2 recycling and hence its availability at cell surface within the dose range studied [31].



**Fig. 3.** *In vitro* tube formation assay of HUVEC cells in response to various study compounds. RGDfK targeted HPMA copolymer-AH-GDM conjugate significantly reduced the number of tubes formed compared to the control group as well as untargeted constructs. For sample characteristics see Table 1. \*P value < 0.05, \*\*P value < 0.01.

### 3.4. Migration inhibition assay

Angiogenesis is a coordinated process that requires not only an increase in the synthesis and deposition of stromal proteins, but also a proliferation and migration of endothelial cells. To assess the effect of RGDfK delivery systems on HUVEC migration, the scratch wound assay was employed. In this assay HUVECs after wounding were incubated with drugs used at the same AH-GDM equivalent concentrations that did not affect cell viability for the duration of the experiment. To rule out possible involvement of targeting moiety, cells also were incubated with free RGDfK and P4 (Table 1) at the concentrations equivalent to the concentration of the peptide added with the targeted conjugate.

Scratch wound assay indicated that HUVECs covered the wounded area almost completely within 24 h post-scratch (Fig. 4A and B). Neither free RGDfK (data not shown) nor P4 (Fig. 4C) affected the rate of wound healing. Similarly, both unconjugated AH-GDM and P1 did not affect the rate of wound healing (Fig. 4D and E) showing that the open area remained after 24 h of cell exposure to the drugs. In contrast to these observations P3 significantly delayed the wound healing process resulting in almost 50% wounded area open after 24 h of cell exposure to the drug (Fig. 4F). The results clearly show that neither AH-GDM nor RGDfK alone were able to inhibit HUVEC migration indicating the advantage of the targeted delivery system compared to the untargeted one in delaying neoangiogenesis.

### 3.5. Anticancer activity of the conjugates in vivo

Prostate cancer is the second leading cause of cancer-related deaths in the United States. Patients with localized disease are usually treated with surgery or radiation, whereas the treatment for patients with a metastatic disease is purely palliative. Hormonal treatment represents the standard therapy for stage IV prostate cancer, but patients ultimately become unresponsive to androgen ablation. The current study is a continuation of our research strategy to develop targeted polymeric delivery systems that can significantly enhance the therapeutic index of prostate cancer chemotherapy. To this end, we have shown that the cyclic integrin targeting peptides (RGDfK) substantially increase the tumor accumulation of *N*-(2-hydroxypropyl)methacrylamide (HPMA) copolymers [22]. This study was conducted to examine the efficacy of RGDfK targeted geldanamycin derivative AH-GDM conjugated to HPMA copolymers compared to untargeted systems. We also compared this neoangiogenic targeting strategy to the well established EPR molecular size based targeting, in terms of tumor growth inhibition in the DU-145 human prostate model in nude mice.

As shown in Fig. 5A, P3 had the highest tumor growth inhibition at both 20, and 60 mg/kg doses respectively. At 60 mg/kg, the growth inhibition by the targeted polymeric conjugate was statistically significant when compared to the control group ( $P < 0.01$ ) and to the non-targeted P1 and P2 conjugates of both small and large molecular weight carriers ( $P < 0.05$ ). Large molecular weight construct P2 (38.7 kDa) showed a trend towards higher tumor efficacy compared to P1 (22.2 kDa), the small molecular weight polymer drug conjugate, however this difference between groups was not statistically significant. Paradoxically, lower dose of the targeted P3, as well as large molecular weight P2 conjugates showed enhanced tumor growth. The RGDfK containing polymer-drug conjugate P3, with molecular weight of 18 kDa (which is below renal excretion threshold), has a much smaller hydrodynamic diameter (3.0 nm) than the 38.7 kDa nontargeted construct (7.3 nm) (Table 1). Nevertheless the targetable system was significantly more effective in controlling tumor growth. This data indicates the value of active targeting of the neovasculature over passive EPR targeting. As shown in Fig. 5B, the constructs used in this experiment had no effect in animal weight as reflected by the steady weight gain of all groups with no statistically

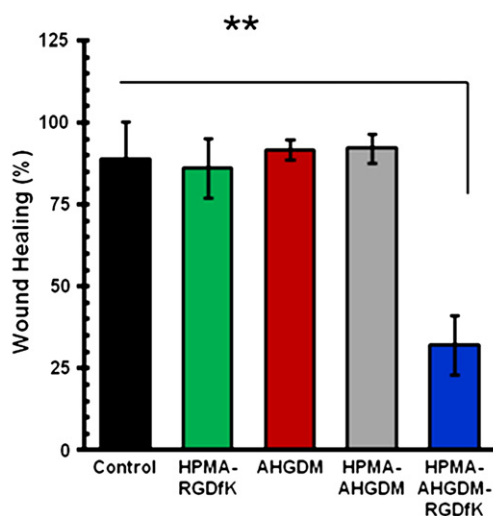
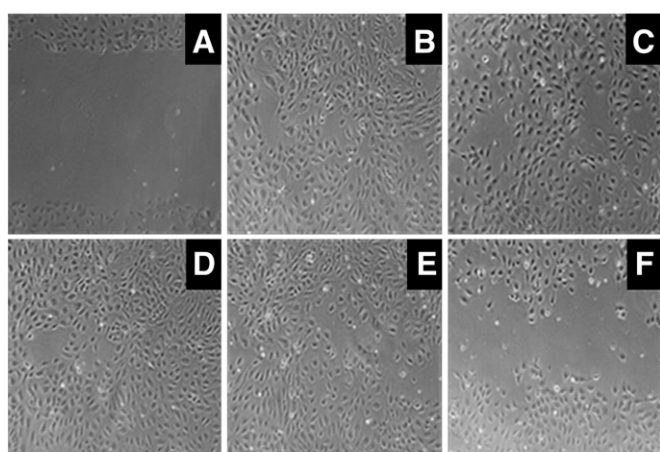


**Fig. 4.** Effect of conjugates on HUVEC migration. Left; Representative photomicrographs of control cells at 1 h (A) and 24 h (B) post-scratch; cells treated with HPMA copolymer-RGDfK (C), AH-GDM (D), HPMA copolymer-AH-GDM (E), and HPMA copolymer-AH-GDM-RGDfK (F) 24 h post-scratch. All samples were used at the concentration equivalent to 3.2  $\mu$ M of AH-GDM. Right; Quantitative analysis of sample effect on wound area healing 24 h post-scratch. Data are presented as mean  $\pm$  S.D. n = 6, \*\*P value < 0.01.

significant difference compared to the control group. It is noteworthy that in this study we could safely inject 60 mg/kg of all the polymeric AH-GDM constructs, substantially higher than the MTD of free AH-GDM.

### 3.6. Antiangiogenic effect of the conjugates

Geldanamycin derivatives including AH-GDM demonstrate potent inhibition of new vessel formation through different mechanisms. GDM binds to Hsp90 and inhibits Hsp90 mediated client protein unfolding. Inactivation of Hsp90 can result in antiangiogenic effect through multiple pathways including inhibiting the antiapoptotic signaling in response to VEGF in endothelial cells [13], antagonistic effect against VEGF-induced endothelial cell migration [32], inhibition of G-protein mediated transduction pathways that lead to the activation of iNOS and consequently to the neoangiogenic effects mediated by nitric oxide [14,15]. In addition, hypoxia-inducible factor (HIF-1 $\alpha$ ) which drives the transcription of VEGF, is essential for angiogenesis [33]. GDM derivatives have shown to inhibit Hsp90 mediated activation, stability, and function of HIF-1 $\alpha$  [11,12]. In our study, tumor size regression in DU-145 tumor bearing mice clearly indicated the advantageous antitumor effect of RGDfK targeted polymer drug conjugates (P3) compared to nontargeted systems

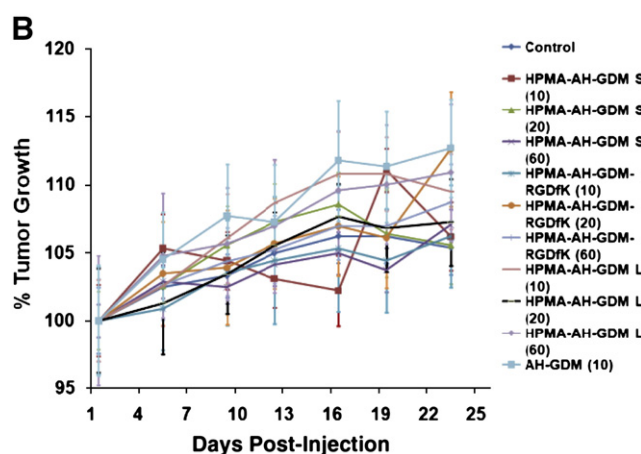
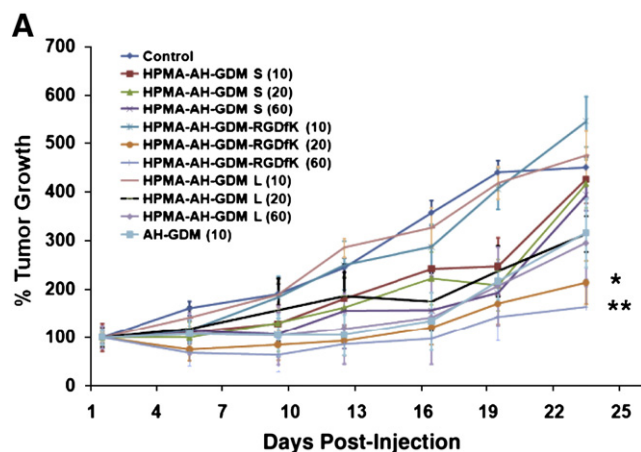


**Fig. 5.** A) Anticancer efficacy of HPMA copolymer-AH-GDM conjugates against DU-145 prostate cancer in nude mice. B) The weight change of nude mice in response to treatment with HPMA copolymers. S; small molecular weight, and L; large molecular weight (see Table 1). \*\*P < 0.01, and \*P < 0.05 compared to control group.

(P1 and P2). In order to correlate the *in vivo* antiangiogenic mechanism with this antitumor effect we used the directed *in vivo* angiogenesis assay [34]. In this assay, we adopted the *in situ* application of various polymeric conjugates studied in the angioreactor at concentrations far below the IC<sub>50</sub> of the AH-GDM contents, to allow for vessel formation and comparison across the study compounds. As shown in Fig. 6, all the compounds under study showed significant suppression of new vessel formation at the dose under investigation compared to the control group or to conjugate P4 not containing AH-GDM. The difference between the study compounds was not statistically significant. Although this result proves the antiangiogenic potential of various constructs with AH-GDM, it does not show any added advantage due to RGDfK targeting. This can be explained by the nature of the assay, where all the study compounds are mixed with the basement membrane extract gel in the angioreactor prior to implantation into the animals, which nullify any targeting advantage that can be provided by the targeting moiety.

### 3.7. Enhancement of tumor permeability in response to HPMA copolymer-geldanamycin-RGDfK conjugates at sub-therapeutic doses

As shown in Fig. 5A, RGDfK targeted P3 had superior anticancer efficacy compared to untargeted P1 constructs at both 20, and 60 mg/kg AH-GDM equivalence. Conversely, 10 mg/kg of targeted polymeric conjugate showed considerable tumor progression that exceeds that of control group. As known for many cytotoxic anticancer agents, sub-therapeutic doses can result in adverse tumor growth. In our study we examined if this effect can be associated with abnormal

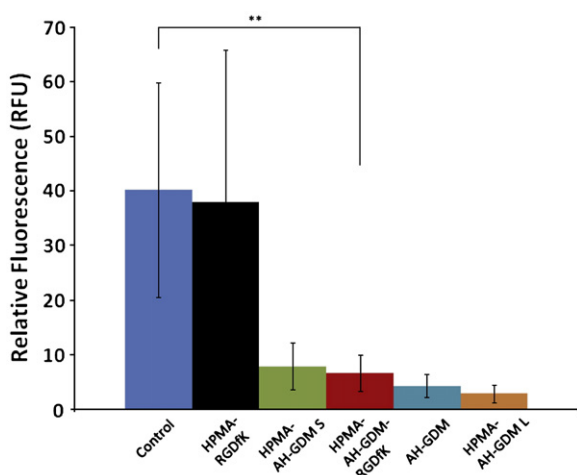


**Fig. 6.** Directed *in vivo* angiogenesis assay in response to polymeric AH-GDM conjugates. After implantation with angioreactors containing basement membrane extract with growth factors for 2 weeks, angioreactors were removed from the mice, cells were collected from basement membrane extract and labeled with FITC-lectin. Then, fluorescence was measured by spectrofluorometry. All AH-GDM-containing polymeric conjugates significantly reduced neoangiogenesis in nude mice compared to the control group. \*\*P value < 0.01 compared to control group.

vascular function. For this study, we used the same model of DU-145 prostate cancer in nude mice, and evaluated the EBD concentration as a model of putative nanomedicine in tumors, 24 h after injection of 10 mg/kg AH-GDM equivalence in mice (Fig. 7).

As shown in Fig. 6, RGDfK targeted P3 conjugates have the highest permeability per tumor gm weight, followed by the large molecular weight constructs, then small molecular weight P1 and finally the unconjugated AH-GDM. This order of enhanced permeability matches the tumor volume in Fig. 5A. One possible explanation that can account for the increased permeability accompanied with the low dose of P3 administration is that, low dose of RGDfK peptide itself can account for the higher permeability. While high dose RGDfK peptides have shown to inhibit tumor angiogenesis [35], low dose of the peptide can enhance the tumor angiogenesis due to promoting the Rab4A-mediated recycling of both  $\alpha_v\beta_3$  integrin and VEGFR2 in

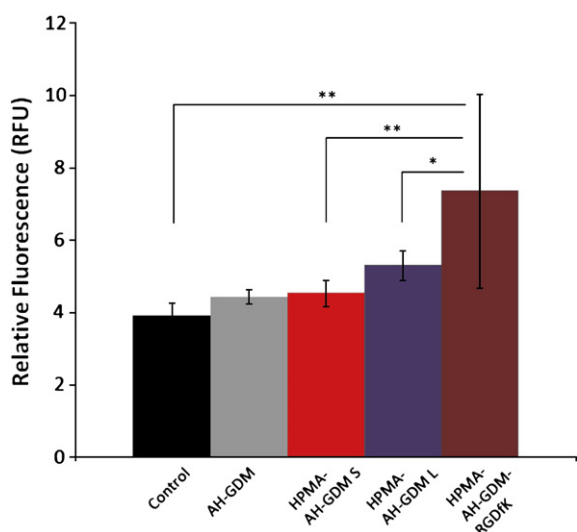


**Fig. 7.** Evans blue dye (EBD) concentration as a model of putative macromolecular drug concentration in DU-145 tumors. At 10 mg/kg AH-GDM equivalent, RGDfK targeted conjugate increased the EBD concentration in tumors by approximately 2 fold greater than the control group. The differences between HPMA copolymer-AH-GDM-RGDfK and control as well as the targeted and untargeted conjugates were statistically significant. \*P value < 0.05, \*\*P value < 0.01.

response to VEGF and hence enhance endothelial cell migration and proliferation [31]. Indeed, when this study was repeated with only the P4 sample high permeability was observed (data not shown). To our knowledge, this is the first report that describes higher permeability of tumor tissue in response to lower doses of RGDfK targeted conjugates. The clinical benefit of exploiting this phenomenon is clear for enhancing the delivery of co-administered drugs with low doses of RGDfK conjugates.

#### 4. Conclusions

This study demonstrates the anticancer efficacy of P3 (RGDfK targeted polymer drug conjugate) and its superior activity over the passive targeting of large molecular weight P2 conjugates. The anticancer effect of study compounds can be attributed at least partially to the antiangiogenic effect of the drug as demonstrated both *in vitro* and *in vivo*. In addition, the enhanced permeability of tumor tissues in response to low doses of RGDfK targeted polymeric constructs is reported. The enhanced permeability of polymeric RGDfK conjugates at lower doses can be exploited as a mechanism for enhancing the delivery of chemotherapeutic agents to solid tumors. The results of the current study warrant exploration of the use of RGDfK targeted drugs for clinical management of prostate cancer.

#### Acknowledgments

The authors thank Michele Grüner for her excellent technical support. This work was supported by the National Institutes of Health (R01-EB007171) and the Utah Science Technology and Research (USTAR) Initiative.

#### References

- [1] J. Folkman, Angiogenesis in cancer, vascular, rheumatoid and other disease, *Nat. Med.* 1 (1) (1995) 27–31.
- [2] G. Neufeld, T. Cohen, S. Gengrinovitch, Z. Poltorak, Vascular endothelial growth factor (VEGF) and its receptors, *FASEB J.* 13 (1) (1999) 9–22.
- [3] A.K. Olsson, A. Dimberg, J. Kreuger, L. Claesson-Welsh, VEGF receptor signalling – in control of vascular function, *Nat. Rev. Mol. Cell Biol.* 7 (5) (2006) 359–371.
- [4] K.M. Cook, W.D. Figg, Angiogenesis inhibitors: current strategies and future prospects, *CA Cancer J. Clin.* 60 (4) (2010) 222–243.
- [5] P.J. Polverini, Cellular adhesion molecules newly identified mediators of angiogenesis, *Am. J. Pathol.* 148 (4) (1996) 1023–1029.
- [6] A. Meyer, J. Auernheimer, A. Modlinger, H. Kessler, Targeting RGD recognizing integrins: drug development, biomaterial research, tumor imaging and targeting, *Curr. Pharm. Des.* 12 (22) (2006) 2723–2747.
- [7] O. Cleaver, D.A. Melton, Endothelial signaling during development, *Nat. Med.* 9 (6) (2003) 661–668.
- [8] C. Derleth, I.A. Mayer, Antiangiogenic therapies in early-stage breast cancer, *Clin. Breast Cancer* 10 (Suppl 1) (2010) E23–E31.
- [9] C. Hwang, E.I. Heath, Angiogenesis inhibitors in the treatment of prostate cancer, *J. Hematol. Oncol.* 3 (2010) 26.
- [10] J.M. Holzbeierlein, A. Windsperger, G. Vielhauer, Hsp90: a drug target? *Curr. Oncol. Rep.* 12 (2) (2010) 95–101.
- [11] J.S. Isaacs, Y.J. Jung, E.G. Mimnaugh, A. Martinez, F. Cuttitta, L.M. Neckers, Hsp90 regulates a von Hippel Lindau-independent hypoxia-inducible factor-1 alpha-degradative pathway, *J. Biol. Chem.* 277 (33) (2002) 29936–29944.
- [12] E. Minet, D. Mottet, G. Michel, I. Roland, M. Raes, J. Remacle, C. Michiels, Hypoxia-induced activation of HIF-1: role of HIF-1alpha-Hsp90 interaction, *FEBS Lett.* 460 (2) (1999) 251–256.
- [13] S. Dias, S.V. Shmelkov, G. Lam, S. Rafii, VEGF(165) promotes survival of leukemic cells by Hsp90-mediated induction of Bcl-2 expression and apoptosis inhibition, *Blood* 99 (7) (2002) 2532–2540.
- [14] G. Garcia-Cardena, R. Fan, V. Shah, R. Sorrentino, G. Cirino, A. Papapetropoulos, W.C. Sessa, Dynamic activation of endothelial nitric oxide synthase by Hsp90, *Nature* 392 (6678) (1998) 821–824.
- [15] A. Brouet, P. Sonveaux, C. Dessy, S. Moniotte, J.L. Balligand, O. Feron, Hsp90 and caveolin are key targets for the proangiogenic nitric oxide-mediated effects of statins, *Circ. Res.* 89 (10) (2001) 866–873.
- [16] D.B. Solit, F.F. Zheng, M. Drobnjak, P.N. Munster, B. Higgins, D. Verbel, G. Heller, W. Tong, C. Cordon-Cardo, D.B. Agus, H.I. Scher, N. Rosen, 17-Allylamino-17-demethoxygeldanamycin induces the degradation of androgen receptor and HER-2/neu and inhibits the growth of prostate cancer xenografts, *Clin. Cancer Res.* 8 (5) (2002) 986–993.

- [17] K. Greish, J. Fang, T. Inutsuka, A. Nagamitsu, H. Maeda, Macromolecular therapeutics: advantages and prospects with special emphasis on solid tumour targeting, *Clin. Pharmacokinet.* 42 (13) (2003) 1089–1105.
- [18] K. Greish, Enhanced permeability and retention of macromolecular drugs in solid tumors: a royal gate for targeted anticancer nanomedicines, *J. Drug Target.* 15 (7–8) (2007) 457–464.
- [19] J. Kopecek, P. Kopeckova, HPMA copolymers: origins, early developments, present, and future, *Adv. Drug Deliv. Rev.* 62 (2) (2010) 122–149.
- [20] R. Duncan, Development of HPMA copolymer-anticancer conjugates: clinical experience and lessons learnt, *Adv. Drug Deliv. Rev.* 61 (13) (2009) 1131–1148.
- [21] E. Segal, R. Satchi-Fainaro, Design and development of polymer conjugates as anti-angiogenic agents, *Adv. Drug Deliv. Rev.* 61 (13) (2009) 1159–1176.
- [22] D.B. Pike, H. Ghandehari, HPMA copolymer-cyclic RGD conjugates for tumor targeting, *Adv. Drug Deliv. Rev.* 62 (2) (2010) 167–183.
- [23] J. Strohalm, J. Kopecek, Poly N-(2-hydroxypropyl)methacrylamide: 4 Heterogeneous polymerization, *Angew. Makromol. Chem.* 70 (1978) 109–118.
- [24] P. Rejmanova, J. Labsky, J. Kopecek, Aminolyses of monomeric and polymeric p-nitrophenyl esters of methacryloylated amino acids, *Makromol. Chem.* 178 (1977) 2159–2168.
- [25] K. Ulbrich, V. Subr, J. Strohalm, D. Plocova, M. Jelinkova, B. Rihova, Polymeric drugs based on conjugates of synthetic and natural macromolecules I. Synthesis and physico-chemical characterisation, *J. Control. Release* 64 (1–3) (2000) 63–79.
- [26] Y. Kasuya, Z.R. Lu, P. Kopeckova, S.E. Tabibi, J. Kopecek, Influence of the structure of drug moieties on the in vitro efficacy of HPMA copolymer-geldanamycin derivative conjugates, *Pharm. Res.* 19 (2) (2002) 115–123.
- [27] M.P. Borgman, A. Ray, R.B. Kolhatkar, E.A. Sausville, A.M. Burger, H. Ghandehari, Targetable HPMA copolymer-aminohexylgeldanamycin conjugates for prostate cancer therapy, *Pharm. Res.* 6 (2009) 1407–1418.
- [28] M.P. Borgman, O. Aras, S. Geysler-Stoops, E.A. Sausville, H. Ghandehari, Biodistribution of HPMA copolymer-aminohexylgeldanamycin-RGDfK conjugates for prostate cancer drug delivery, *Mol. Pharm.* (2009).
- [29] K. Mulgrew, K. Kinneer, X.T. Yao, B.K. Ward, M.M. Damschroder, B. Walsh, S.Y. Mao, C. Gao, P.A. Kiener, S. Coats, M.S. Kinch, D.A. Tice, Direct targeting of alphavbeta3 integrin on tumor cells with a monoclonal antibody, *Abegrin Mol Cancer Ther* 5 (12) (2006) 3122–3129.
- [30] G.E. Davis, D.R. Senger, Endothelial extracellular matrix: biosynthesis, remodeling, and functions during vascular morphogenesis and neovessel stabilization, *Circ. Res.* 97 (11) (2005) 1093–1107.
- [31] A.R. Reynolds, I.R. Hart, A.R. Watson, J.C. Welti, R.G. Silva, S.D. Robinson, G. Da Violante, M. Gourlaouen, M. Salih, M.C. Jones, D.T. Jones, G. Saunders, V. Kostourou, F. Perron-Sierra, J.C. Norman, G.C. Tucker, K.M. Hodivala-Dilke, Stimulation of tumor growth and angiogenesis by low concentrations of RGD-mimetic integrin inhibitors, *Nat. Med.* 15 (4) (2009) 392–400.
- [32] S. Rousseau, F. Houle, H. Kotanides, L. Witte, J. Waltenberger, J. Landry, J. Huot, Vascular endothelial growth factor (VEGF)-driven actin-based motility is mediated by VEGFR2 and requires concerted activation of stress-activated protein kinase 2 (SAPK2/p38) and geldanamycin-sensitive phosphorylation of focal adhesion kinase, *J. Biol. Chem.* 275 (14) (2000) 10661–10672.
- [33] G.L. Semenza, Hypoxia-inducible factor 1: oxygen homeostasis and disease pathophysiology, *Trends Mol. Med.* 7 (8) (2001) 345–350.
- [34] L. Guedez, A.M. Rivera, R. Salloum, M.L. Miller, J.J. Diegmüller, P.M. Bungay, W.G. Stetler-Stevenson, Quantitative assessment of angiogenic responses by the directed in vivo angiogenesis assay, *Am. J. Pathol.* 162 (5) (2003) 1431–1439.
- [35] R.E. Nisato, J.C. Tille, A. Jonczyk, S.L. Goodman, M.S. Pepper, Alpha v beta 3 and alpha v beta 5 integrin antagonists inhibit angiogenesis in vitro, *Angiogenesis* 6 (2) (2003) 105–119.